journal of materials processing technology 209 (2009) 3444–3451

journal homepage: www.elsevier.com/locate/jmatprotec

Microstructural characterizations of magnetron sputtered Ti films on glass substrate

Vipin Chawla[a,b], *R. Jayaganthan*[a,*], *A.K. Chawla*[b], *Ramesh Chandra*[b]

[a] *Department of Metallurgical and Materials Engineering & Centre of Nanotechnology, Indian Institute of Technology Roorkee, Roorkee 247667, India*

[b] *Nano Science Laboratory, Institute Instrumentation Centre, Indian Institute of Technology Roorkee, Roorkee 247667, India*

ARTICLE INFO

Article history:
Received 6 January 2008
Received in revised form
10 July 2008
Accepted 2 August 2008

Keywords:
Ti thin films
Sputtering
Microstructural characterization

ABSTRACT

Magnetron sputtered Ti thin films deposited on glass substrates under varying deposition parameters were characterized by X-Ray Diffraction, Scanning Electron Microscopy and Atomic Force Microscopy. The textures of the Ti films characterized by X-ray diffraction revealed the initial (1 0 0) preferred orientation but it transformed in to (0 0 2) and (1 0 1) orientation with increase in sputtering power and substrate temperature, respectively. The preferred orientations of (0 0 2) and (1 0 1) were observed for the films deposited with the sputtering pressure of 5 mTorr and 20 mTorr, respectively. The average surface roughness of the Ti films showed an increasing trend with power, pressure, and temperature from the Atomic Force Microscopy analysis. The dense film morphology was observed in the Scanning Electron Microcopy images of Ti thin films deposited with higher substrate temperature (500 °C). X-ray diffraction analysis revealed that the grain size of the Ti thin films exhibits an increasing trend with varying deposition parameters.

© 2008 Elsevier B.V. All rights reserved.

1. Introduction

Ti thin films are used in biomedical and diffusion barrier applications due to their superior strength, excellent thermal and chemical stability (Boyer, 1996; Textor et al., 2001; Shoesmith et al, 1997a,b). The microstructural characteristics such as grain size, morphology, density and textures of the grains strongly influence the structural and functional properties of Ti thin films. Therefore, it is very essential to understand the influence of process parameters on the microstructural characteristics of the Ti thin films to further enhance their properties in the actual applications (Cai et al., 2005; Jeyachandran et al., 2006; Jung et al., 2003). Ti thin films with the enhanced strength, biocompatibility and adhesion behavior could be better substitute for Ti-based nitride coatings used in the biomedical applications.

The chemical and structural characteristics of Ti coatings were investigated in the earlier work (Ogawa et al., 1991; Iida, 1990). Jeyachandran et. al (Jeyachandran et al., 2006) have investigated the properties of Ti-films deposited by DC-magnetron sputtering and reported the formation of amorphous and crystalline films under different processing conditions. The films were uniform and densely packed with smooth surface roughness as well as shown the potential of DC-magnetron sputtering technique to prepare metallic and crystalline Ti films at a base pressure of 4×10^{-4} Pa, cathode power in the range of 125–150 W and sputtering pressure ranging from 1.1 Pa to 2 Pa. The Ti thin films processed by magnetron sputtering and grid attached magnetron

* *Corresponding author*. Tel.: +91 1332 285869; fax: +91 1332 285243.
E-mail address: rjayafmt@iitr.ernet.in (R. Jayaganthan).
0924-0136/$ – see front matter © 2008 Elsevier B.V. All rights reserved.
doi:10.1016/j.jmatprotec.2008.08.004

sputtering were investigated and reported the formation of (1 0 0) and (0 0 2) preferred orientation of the grains in the Ti films, with increase in bias voltage, in these two sputtering techniques (Jung et al., 2003), respectively. The films deposited using grid attached magnetron sputtering resulted in dense structure with a smooth, specular reflecting surface with increased flux of Ti ions. Godfroid et al. (2003) have studied the growth of ultra thin Ti films deposited on SnO_2 by magnetron sputtering. The growth mode of Ti thin films has changed from Volmer Weber mode for a low deposition rate to a pseudo Frank van der Merwe mode with the increase in deposition rate. Siva Rama Krishna and Sun (2005) have investigated the influence of thermal oxidation conditions on the tribological behavior of Ti films on stainless steel and concluded that the films transforms into Rutile (TiO_2) resulting in three layer hybrid structures. The nanostructured Ti thin films on (0 0 1) Si substrate were deposited by ion beam sputtering technique and shown (Muraishi et al., 2004) that as deposited films exhibited hcp structure with [0 0 0 1] textured grains. Pulsed magnetron sputtering has been used to deposit Ti and TiO_2 films, in the literature (Henderson et al., 2003), and found that the films exhibited improved adhesion and surface roughness as compared to DC sputtering. Martin et al. (1998) have investigated the effect of bias power on Ti films prepared by RF magnetron sputtering. AFM analysis of the Ti films in their work revealed a change in surface topography of the films and reduction of surface roughness and erosion process with increasing bias power treatment. Ko et al. (1999) have investigated the microstructural features of Ti films formed, on p-type (0 0 1) single crystal Si wafer, by the ionized sputtering process and revealed the formation of the less strong (0 0 2) textures in the films, without the substrate bias, when compared to collimated sputtering. The residual stress and structural characteristics of Ti films on glass substrates deposited by planar magnetron sputtering were carried out by Savaloni et al. (2004) and they reported that the grain size increase was dependent on the substrate temperature and film thickness. The films exhibited (1 0 0) preferred orientation as observed in their work. The surface structure and composition of flat Ti thin films, deposited by e-beam evaporation technique, on glass substrate were characterized by AFM and XPS, respectively (Cai et al., 2005). A direct linear relationship between surface roughness and evaporation rate was observed using AFM characterization. The films with larger grains are correlated with root mean square surface roughness. Vijaya et al. (1996) have characterized the bias assisted magnetron sputtered Ti films on glass substrates by XRD and TEM and observed the reduction in grain size of the films with increasing bias voltage. They observed the fcc phase transformation in Ti thin films from its SAED patterns and it was attributed to the formation of oxide phase due to presence of trace amounts of water vapor or residual gases during deposition.

The systematic investigation and quantification of the influence of each of the process parameters on the microstructural features of Ti thin films are essential for enhancing its strength and adhesion in biomedical and microelectronics applications. Owing to these facts, the present work has been focused to deposit Ti films on glass substrate by DC Magnetron Sputtering and characterize their microstructural features by XRD, FE-SEM, and AFM. The influence of process parameters such as sputtering power, substrate temperature and sputtering pressure on the texture of Ti films has been investigated in the present work.

2. Experimental details

2.1. *Processing of Ti films*

The Ti films were deposited by DC magnetron sputtering onto glass substrates using a 99.99% pure titanium target (2 in. diameter and 5-mm thick). The substrates were cleaned by rinsing in ultrasonic baths of acetone and methanol and dried under nitrogen gas. The base pressure was better than 2×10^{-6} Torr and the sputtering was carried out in an Argon atmosphere. The deposition time was kept constant while sputtering power, substrate temperature and sputtering pressure were varied from 50–150 W, 100–500 °C and 5–20 mTorr, respectively. The substrate temperature and sputtering pressure were kept constant at 100 °C and 10 mTorr respectively when sputtering power is varied, while during temperature variation, sputtering power and sputtering pressure were kept constant at 50 W and 10 mTorr respectively and during sputtering pressure variation, sputtering power and substrate temperature were kept constant at 50 W and 100 °C, respectively. Before starting the actual experiment, the target was pre-sputtered for 15 min with a shutter located in between the target and the substrate. This shutter is also used to control the deposition time. The target-substrate distance was kept at 50 mm, during deposition.

2.2. *Characterization details*

The Ti films deposited on glass substrate were first characterized by XRD (Bruker AXS) with Cu Kα X-ray (for the phase identification, grain size measurement and texture analysis). The scan rate used was 1° $\min^{-1}$. and the scan range was from 30 to 45°. The grain size of the Ti films was estimated from the Scherrer's formula, as given in Eq. (1). The grain size '*t*' is along the surface normal direction, which is also the direction of the XRD diffraction vector.

$$t = \frac{0.9\,\lambda}{B\cos\theta} \qquad (1)$$

where *B* (crystallite) is the corrected full-width at half maximum (FWHM) of a Bragg peak, λ is the wavelength of X-ray, and θ is the Bragg angle. B is obtained by the equation $B^2 = B_r{}^2 - B^2{}_{strain} - C^2$ (Warren and Biscce, 1938), where B_r is the FWHM of a measured Bragg peak, $B_{strain} = \varepsilon \tan\theta$ is the lattice broadening from the residual strain ε measured by XRD using $\cos^2\alpha \sin^2\Psi$ method and C is the instrumental line broadening. The grain size is measured using the preferred orientation of XRD peaks obtained for the Ti films on glass substrate.

The surface topographical characterizations of the Ti films were obtained from FE-SEM (FEI, Quanta 200F) at an acceleration voltage of 20 KV. The surface morphology of the Ti films was also characterized using AFM (NT-MDT, Ntegra) operated in semi-contact (tapping) mode.

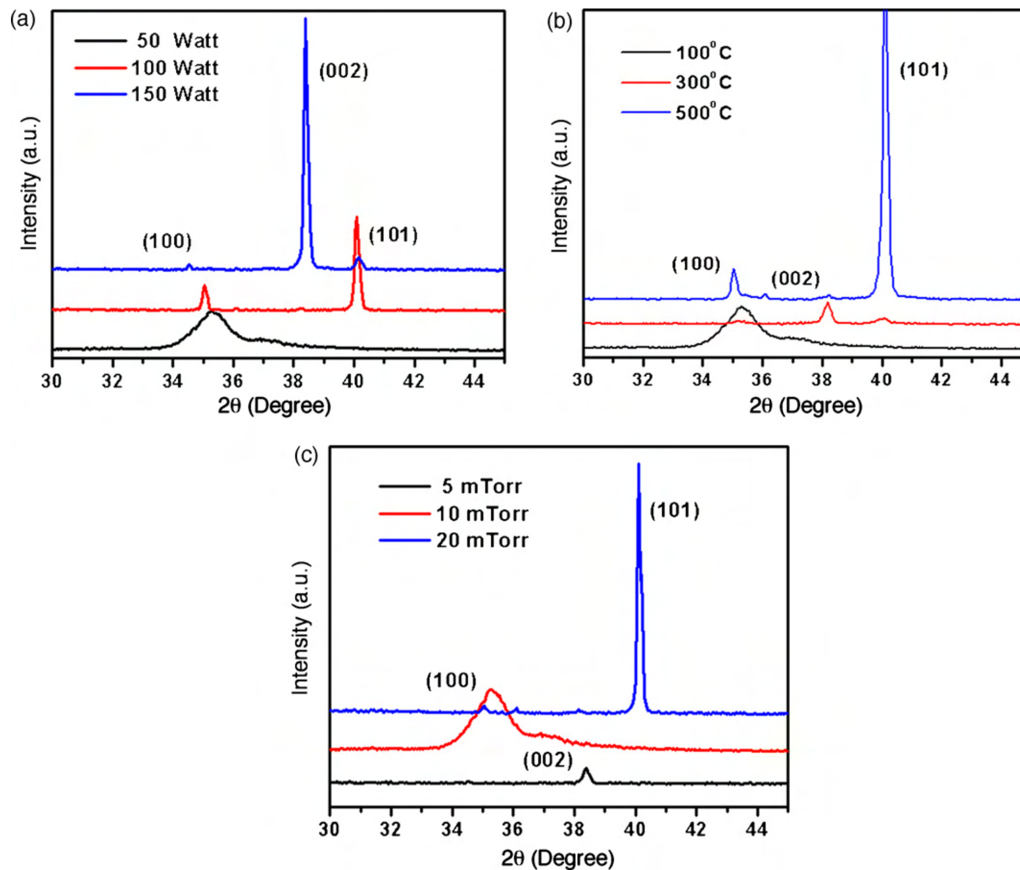

Fig. 1 – XRD graphs of Ti films on glass substrates as a function of (a) sputtering power (b) substrate temperature and (c) sputtering pressure.

3. Results and discussions

The XRD graphs of Ti films deposited at varying sputtering power, substrate temperature and sputtering pressure are plotted in Fig. 1(a)–(c), respectively. In case of varying sputtering power, it is observed that initially the Ti film exhibit (1 0 0) preferred orientation (Fig. 1(a)) but with increasing power (0 0 2) becomes the preferred orientation. However, with increase in the substrate temperature, the initial (1 0 0) orientation subsides and (1 0 1) orientation emerges as the preferred orientation. The XRD results of the Ti films with varying sputtering power may be interpreted on the basis of stress and strain evolution mechanism. The compressive stress induced in the films contributes to the development of (1 0 0) orientation and it may have relaxed to tensile mode at higher thickness favoring the (0 0 2) preferred orientation. The micro strain from (1 0 0) peak of Ti films on glass substrate was calculated by the following equation (Ong et al., 2002; Singh and Kaur, 2008) and shown in Table 1.

$$\alpha = \frac{(\sigma - \sigma_0)}{\sigma_0} \times 100 \qquad (2)$$

Table 1 – Influence of deposition parameters on crystallite size, surface roughness, and microstrain of Ti thin films

S. No.	Parameters	Crystallite size (XRD) (nm)	Average roughness (AFM) (nm)	Film thickness (μm)	Microstrain (1 0 0) peak
(I)	50 Watt	6.4	23.7	3.12	−0.6777
	100 Watt	46.4	101.6	4.76	0.0745
	150 Watt	52.0	194.9	6.49	0.0895
(II)	100 °C	6.4	23.7	3.12	−0.6777
	300 °C	30.8	105.1	3.27	−0.4473
	500 °C	41.8	126.4	3.48	0.0779
(III)	5 mTorr	5.6	13.5	2.14	–
	10 mTorr	6.4	23.7	3.12	−0.6777
	20 mTorr	39.7	95.6	4.35	0.0474

where σ (a or c) is the lattice parameter of the strained Ti films calculated from XRD data and σ_0 (a_0 or c_0) is the unstrained lattice parameter of Ti ($a = 2.9512$ Å and $c = 4.6845$ Å) (Cullity and Stock, 2001). The lattice parameters 'a' and 'c' of Ti films were calculated using the equation (Cullity and Stock, 2001):

$$\frac{1}{d^2} = \frac{4}{3}\frac{(h^2 + hk + k^2)}{a^2} + \frac{l^2}{c^2} \quad (3)$$

where d is the interplanar distance obtained from the position of the (1 0 0) peak using the Bragg condition, a and c are the lattice parameters (being hexagonal structure $c/a = \sqrt{8/3}$) and h, k and l are planes. It has been observed that with increasing sputtering power, substrate temperature and sputtering pressure, micro strain was initially negative and then became positive with a corresponding change in crystallite size as shown in Table 1. It may be mentioned that with increase in power, the deposition rate increases, which in turn increases the thickness of the deposited film (Jeyachandran et al., 2007). Similarly, the peak change due to the increase in substrate temperature causes the increase of (1 0 1) orientation while the (0 0 2) orientation decreased at a higher temperature (Sonoda et al., 2004). The higher substrate temperature could facilitate the enhanced mobility of adatoms in the film surface and favored the formation of (1 0 1) orientation of grains. It is evident from the Fig. 1(c) that the (0 0 2) peak appeared at 5 mTorr has transformed into (1 0 1) preferred orientation at 20 mTorr. The competition between strain energy and surface free energy affecting the textures of the grains are heavily dependent on the deposition parameters such as substrate temperature, power and sputtering pressure. The thermal stress induced in the thin films at higher substrate temperature might have also contributed to the modification of (0 0 2) preferred orientation, favoring the formation of (1 0 1) grains. The thermal stress of Ti thin films deposited on glass substrate as a function of deposition temperature has been investigated in our earlier work (Chawla et al., 2008a) by finite element analysis and observed that the induced thermal stress was due to the higher substrate temperature and thermal expansion mismatch between the films and glass substrate. The induced thermal stress in Ti thin film has also been reported in the literature (Savaloni et al., 2004; Sonoda et al., 2004; Naoe et al., 1991).

The texture coefficients of Ti films on glass substrates as a function of different parameters are calculated from its XRD peaks using the following formula (Chawla et al., 2008b) and shown in Fig. 2(a–c).

$$\text{Texture coefficient } (T) = \frac{I(h\,k\,l)}{[I(1\,0\,0) + I(0\,0\,2) + I(1\,0\,1)]} \quad (4)$$

where hkl represents (1 0 0) or (0 0 2) or (1 0 1) orientation. It is observed from Fig. 2(a) that the texture coefficient of (1 0 0) orientation is high, with the sputtering power of 50 W, as

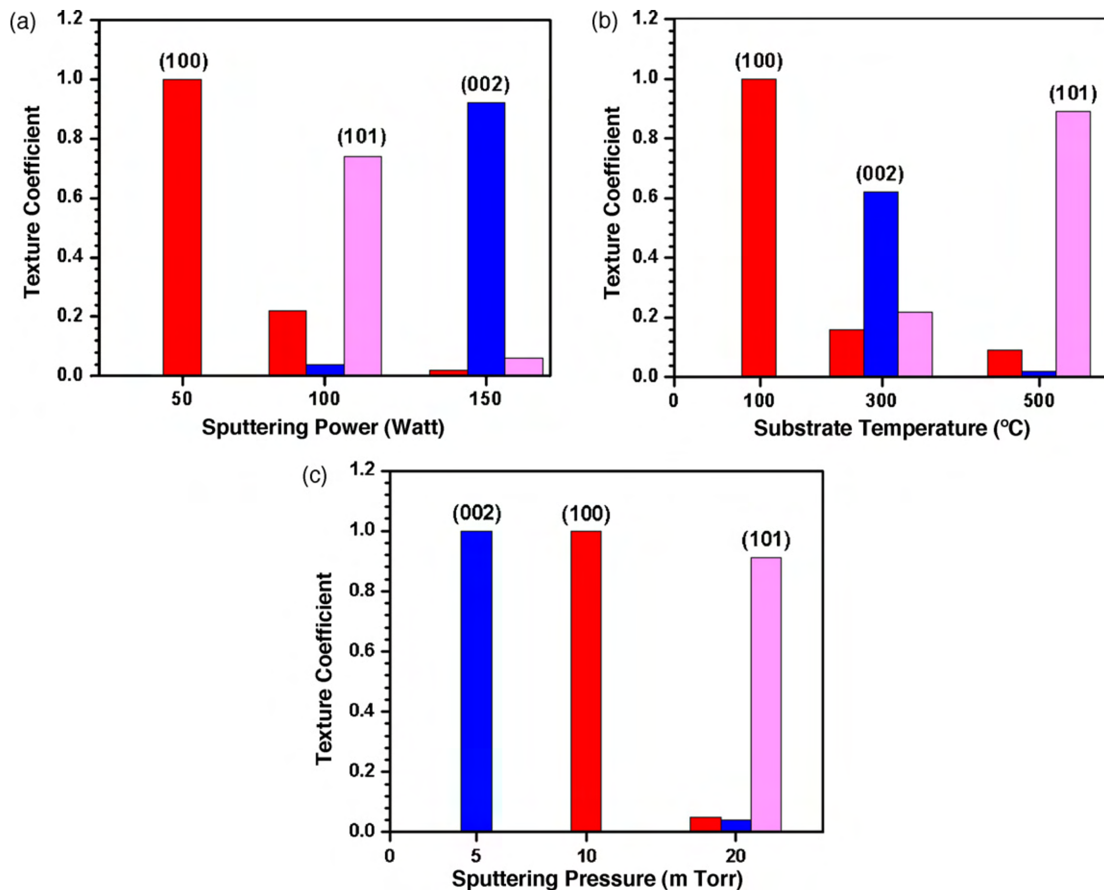

Fig. 2 – Texture coefficients of Ti films on Glass substrates as a function of (a) sputtering power (b) substrate temperature and (c) sputtering pressure.

compared to other orientations. However, (1 0 1) and (0 0 2) orientations exhibit higher values of texture coefficient with increasing sputtering power of 100 W and 150 W, respectively. With varying substrate temperature (Fig. 2(b)), the (1 0 0) orientation showed a higher texture coefficient at 100 °C as compared to other orientations. With increasing temperature, (0 0 2) and (1 0 1) orientations exhibit a higher texture coefficients at 300 °C and 500 °C, respectively. It is shown in Fig. 2(c), with varying sputtering pressure, that the (0 0 2) orientation showed a higher texture coefficient at 5 mTorr as compared to other orientations. With increasing pressure, (1 0 0) and (1 0 1) orientations exhibit a higher texture coefficients at 10 mTorr and 20 mTorr, respectively. The process conditions such as substrate temperature, sputtering pressure and power influ-

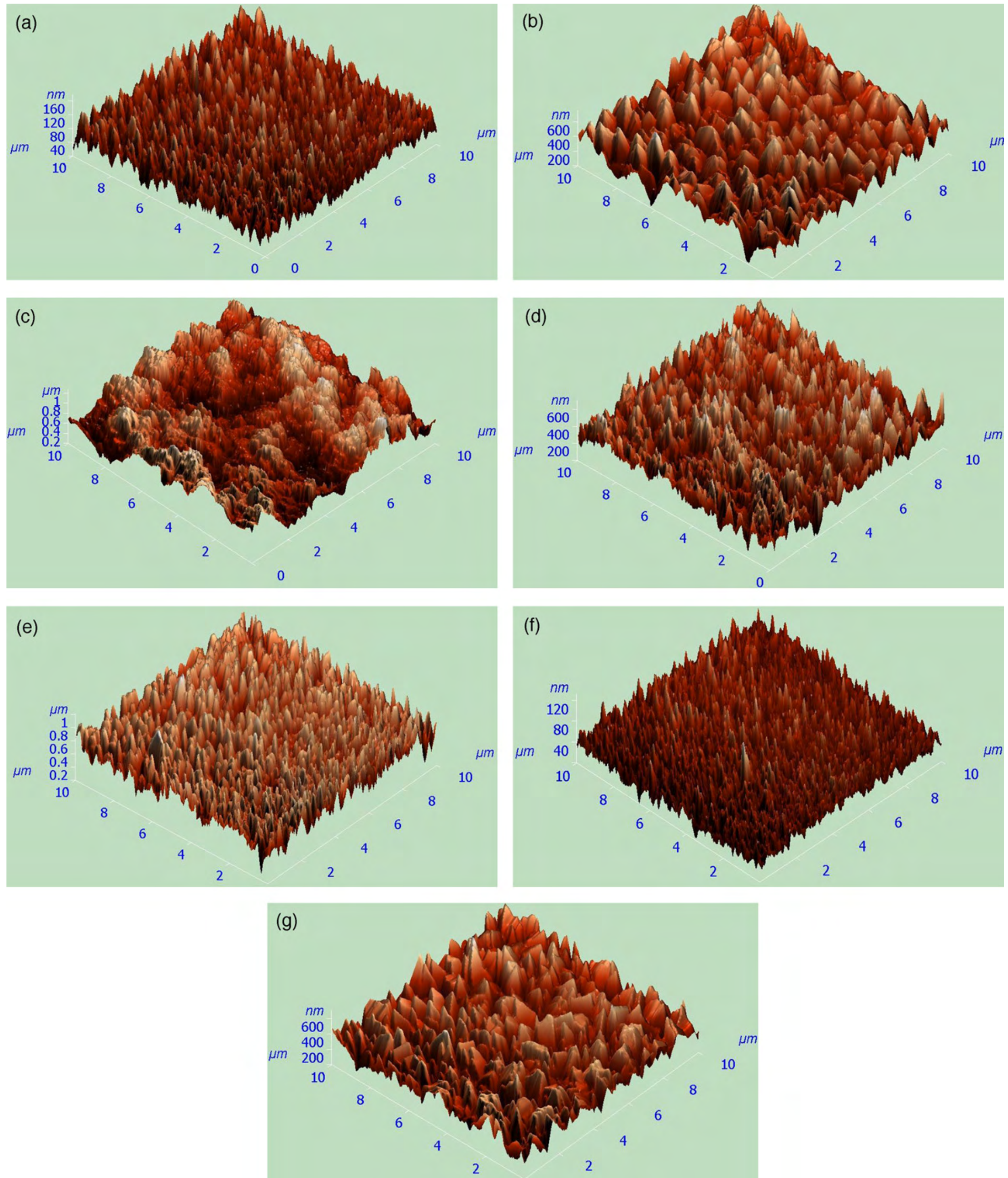

Fig. 3 – AFM images of Ti films on glass substrates as a function of different parameters: (I) sputtering power (a) at 50 W (b) 100 W and (c) at 150 W; (II) substrate temperature (d) at 300 °C and (e) at 500 °C; (III) sputtering pressure (f) at 5 mTorr and (g) at 20 mTorr.

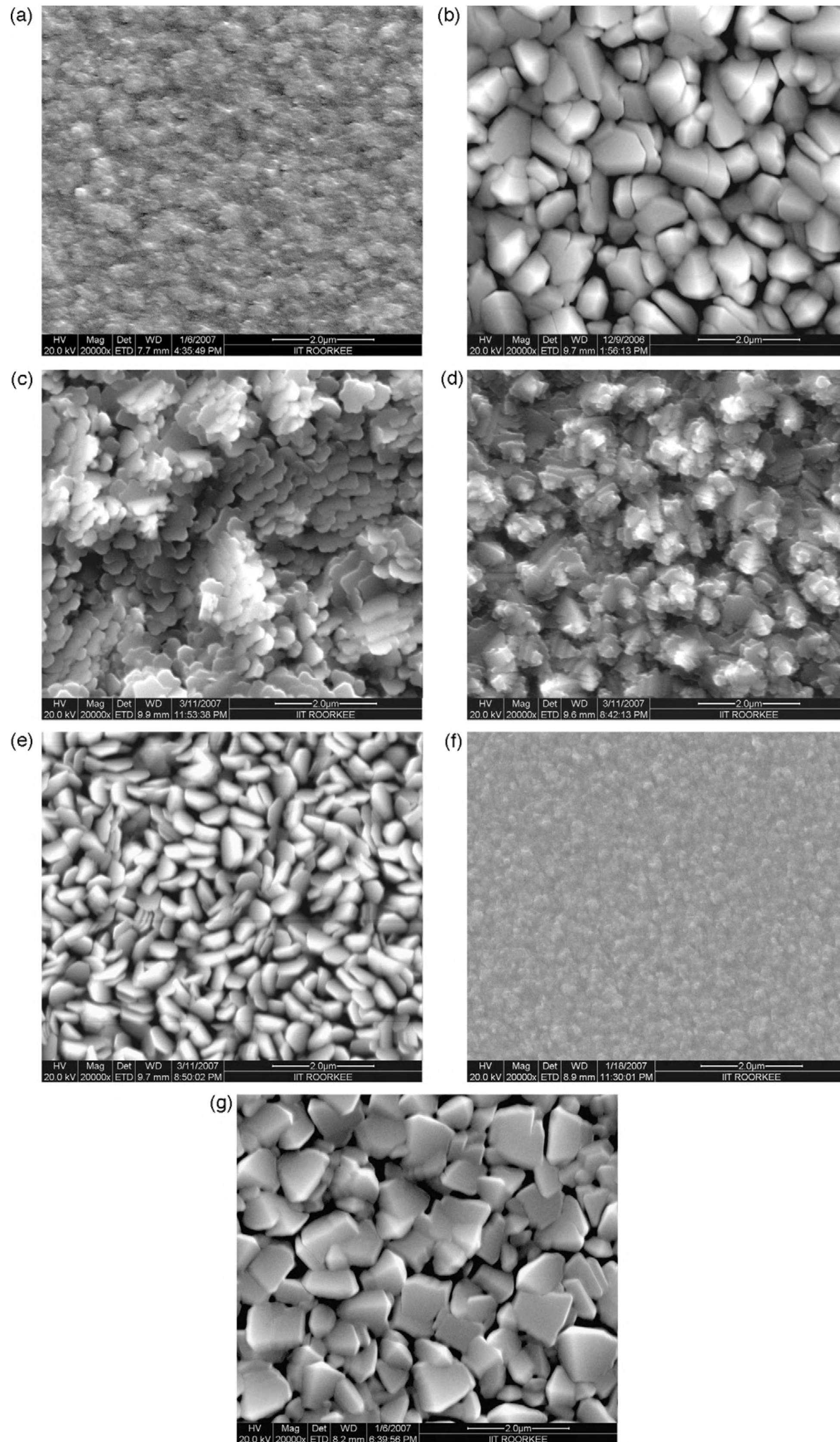

Fig. 4 – FE-SEM images of Ti films on glass substrates as a function of different parameters: (I) sputtering power (a) at 50 W, (b) at 100 W and (c) at 150 W; (II) substrate temperature (d) at 300 °C and (e) at 500 °C; (III) sputtering pressure (f) at 5 mTorr and (g) at 20 mTorr.

ence the surface energy and strain energy of grains formed in the thin films. The competition between surface energy and strain energy during film growth might contribute to the changes in texture of the grains as observed in the present work. The influence of substrate temperature on the microstrains of the Ti thin films is evident from the Table 1. For sufficiently thin films, surface and interface energy minimizing textures are favored but for the thicker films with higher elastic strains, strain energy minimizing textures are formed as reported by Thompson (2000).

The AFM images of Ti films deposited at varying sputtering power are in Fig. 3(a–c). The images of Ti films were acquired in a 10 μm × 10 μm area. It is observed the grain size and surface roughness of Ti films increases with increase in sputtering power. The AFM images of Ti films deposited at varying substrate temperature are shown in Fig. 3(d–e). With increase in substrate temperature, the grain size and surface roughness increase and the morphology of the grains become more crystalline. Fig. 3(f–g) shows the AFM image of the Ti films deposited at sputtering pressure of 5 mTorr and 20 mTorr, respectively. The regular hexagonal crystals are observed for the films deposited at 20 mTorr. The surface roughness exhibits an increasing trend with the sputtering pressure. The crystallite size and surface roughness of Ti thin films deposited with varying power, substrate temperature and sputtering pressure are shown in Table 1. The increase in surface roughness of Ti thin films with higher substrate temperature is due to growth of grains with preferred orientations dictated by surface and grain boundary diffusivity, adatom mobility, film thickness and induced thermal stress (Naeem et al., 1995; Savaloni et al., 2004). The effect of sputtering pressure can be explained by the relationship of the mean free path, λ (cm), with the molecular diameter of the sputtering gas as given by

$$\lambda = 2.330 \times 10^{-20} \frac{T}{(P\delta_m^2)} \tag{5}$$

where T (K) is the temperature, P (Torr) is the sputtering pressure and δ_m (cm) is the molecular diameter (Maissel and Glang, 1970; Chandra et al., 2005). According to above equation when sputtering pressure is high, the mean free path is less so that the sputtered atoms undergo a large number of collisions as a result, the sputtered atoms have a higher probability of agglomeration, i.e. increasing in particle size before arriving at the substrate surface and hence increase in surface roughness of Ti films. With increase in sputtering power, adatom mobility and the deposition rate increases, contributing to growth of crystallite size and higher surface roughness of Ti thin films.

The FE-SEM images of Ti films deposited at varying sputtering power (50 W, 100 W and 150 W), fixed substrate temperature 100 °C and sputtering pressure 10 mTorr are shown in Fig. 4(a–c). With increasing power, the density of the film has increased with lesser fraction of voids due to the higher adatom mobility. Fig. 4(d–e) shows the FE-SEM images of Ti films deposited at varying substrate temperature. The sputtering power and pressure were kept constant at 50 W and 10 mTorr when the substrate temperature was varied from 100 °C to 500 °C. It is evident that with the increase in substrate temperature, the morphology of grain changes and becomes denser due to the higher surface and bulk diffusivity of sputtered atoms. The Ti films deposited at 5 mTorr (Fig. 4f) revealed fine grain morphology as compared to the columnar grains with voids observed for the films deposited at 20 mTorr (Fig. 4g). The morphology of Ti thin films deposited under varying sputtering power, substrate temperature and sputtering pressure are in accordance with the structural zone models discussed in the literature (Thornton, 1977). For example, Ti films deposited with T_s/T_m ratio 0.06 showed a less dense morphology (Zone I) with the voided grain boundaries (Fig. 4b and g) but with T_s/T_m ratio of 0.3, density of the films have increased (Fig. 4e). As discussed in Savaloni's work (2004), the increase in substrate temperature ($T_s/T_m > 0.3$) may lead to the denser film.

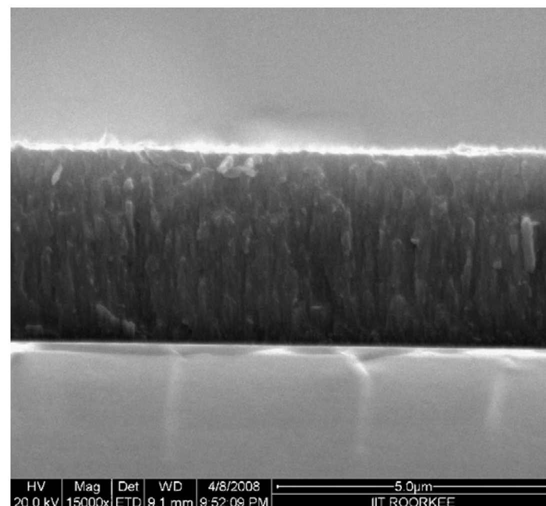

Fig. 5 – Cross-sectional FESEM image of Ti film on glass substrate.

The thickness of the Ti films was measured by taking cross-sectional view of Ti films by FE-SEM and image is shown in Fig. 5 and the thickness data of all Ti film samples are given in Table 1.

4. Conclusion

The effects of sputtering power, substrate temperature and sputtering pressure on the microstructural morphologies of the Ti films deposited by DC-Magnetron sputtering were investigated in the present work. XRD analysis of the textures of the Ti films, deposited under different conditions, revealed the initial (1 0 0) preferred orientation but the (0 0 2) and (1 0 1) orientations were observed with the increasing sputtering power and substrate temperature, respectively. The development of (1 0 0) orientation was due to the compressive stress induced in the films but it transformed into (0 0 2) preferred orientation at higher thickness. The (0 0 2) and (1 0 1) preferred orientations were observed for the films deposited with the sputtering pressure of 5 mTorr and 20 mTorr, respectively. The textures of the films were affected due to the competition between strain energy and surface free energy during deposition of thin films under various process conditions such as substrate tem-

perature, power and sputtering pressure. The thermal stress induced in the thin films at higher substrate temperature has also contributed to the formation of preferred (1 0 1) orientation. The microstrain of Ti films was initially negative and then changed to positive value with increasing sputtering power, substrate temperature, and sputtering pressure. The crystallite size has increased with increase in microstrain in the films. The average surface roughness calculated from the AFM images of the films has shown an increasing trend with varying deposition parameters. The increase in surface roughness of Ti thin films with higher substrate temperature was due to growth of grains with preferred orientations dictated by surface and grain boundary diffusivity, adatom mobility, film thickness and induced thermal stress. The calculated grain size of Ti thin films using XRD results revealed an increasing trend with varying deposition parameters. The uniform and dense morphology of the Ti films were observed with the higher substrate temperature and sputtering pressure as observed from the FE-SEM characterization. The denser morphology of grains observed at higher substrate temperature is due to the higher surface and bulk diffusivity of sputtered atoms.

Acknowledgements

Dr. Ramesh Chandra and Mr. Vipin Chawla, would like to thank DST and DRDO, India, for their financial support to this work.

REFERENCES

Boyer, R.R., 1996. An overview on the use of titanium in the aerospace industry. Mater. Sci. Eng. A 213, 103–114.

Cai, K., Muller, M., Bossert, J., Rechtenbach, A., Jandt, K.D., 2005. Surface structure and composition of flat titanium thin films as a function of film thickness and evaporation rate. Appl. Surf. Sci. 250, 252–267.

Chawla, V., Jayaganthan, R., Chandra, R., 2008a. Finite element analysis of thermal stress in magnetron sputtered Ti coating. J. Mater. Process. Technol. 200, 205–211.

Chawla, V., Jayaganthan, R., Chandra, R., 2008b. Structural characterizations of magnetron sputtered nanocrystalline TiN thin films. Mater. Charact. 59, 1015–1020.

Chandra, R., Chawla, A.K., Kaur, D., Ayyub, P., 2005. Structural, optical and electronic properties of nanocrystalline TiN films. Nanotechnology 16, 053–3056.

Cullity, B.D., Stock, S.R., 2001. Elements of X-ray Diffraction, third ed. Prentice Hall.

Godfroid, T., Gouttebaron, R., Dauchot, J.P., Leclere, Ph., Lazzaroni, R., Hecq, M., 2003. Growth of ultra thin Ti films deposited on SnO_2 by magnetron sputtering. Thin Solid Films 437, 57–62.

Henderson, P.S., Kelly, P.J., Amell, R.D., Backer, H., Bradley, J.W., 2003. Investigation into the properties of titanium based films deposited using pulsed magnetron sputtering. Surf. Coat. Technol. 174-175, 779–783.

Iida, S., 1990. Observation of the surface and structure of very thin Ti film. Jpn. J. Appl. Phys. 29, L361–L363.

Jeyachandran, Y.L., Karunagaran, B., Narayandass, Sa.K., Mangalaraj, D., Jenkins, T.E., Martin, P.J., 2006. Properties of titanium thin films deposited by dc magnetron sputtering. Mater. Sci. Eng. A 431, 277–284.

Jeyachandran, Y.L., Narayandass, Sa.K., Mangalaraj, D., Sami Areva, J.A., Mielczarski, 2007. Properties of titanium nitride films prepared by direct current magnetron sputtering. Mater. Sci. Eng. A 445-446, 223–236.

Jung, M.J., Nam, K.H., Shaginyan, L.R., Han, J.G., 2003. Deposition of Ti thin film using the magnetron sputtering method. Thin Solid Films 435, 145–149.

Ko, D.H., Kim, E.H., Choi, S., Yoo, B.Y., Lee, H.D., 1999. Microstructure analyses of the titanium films formed by the ionized sputtering process. Thin Solid Films 340, 13–17.

Maissel, L.I., Glang, R., 1970. Handbook of Thin Film Technology. McGraw-Hill, New York, p. 1–22.

Martin, N., Baretti, D., Rousselot, C., Rauch, J.Y., 1998. The effect of bias power on some properties of titanium and titanium oxide films prepared by r.f. magnetron sputtering. Surf. Coat. Technol. 107, 172–182.

Muraishi, S., Aizawa, T., Kuwahara, H., 2004. Fabrication of nanostructured titanium thin films via N ion implantation and post annealing treatment. Surf. Coat. Technol. 188–189, 260–264.

Naeem, M.D., Orr-Arienzo, W.A., Rapp, J.G., 1995. Effect of Ti deposition temperature on $TiSi_x$ resistivity. Appl. Phys. Lett. 66 (7), 877–878.

Naoe, M., Ono, S., Hirata, T., 1991. Crystal orientation in titanium thin films deposited by the sputtering method without plasma damage. Mater. Sci. Eng. A 134, 1292–1295.

Ogawa, S., Kousaki, T., Yoshida, T., Sinclair, R., 1991. Interface microstructure of titanium thin-film/silicon single-crystal substrate correlated with electrical barrier heights. J. Appl. Phys. 70, 827–832.

Ong, H.C., Zhu, A.X.E., Du, G.T., 2002. Dependence of the excitonic transition energies and mosaicity on residual strain in ZnO thin films. Appl. Phys. Lett. 80, 941–943.

Savaloni, H., Taherizadeh, A., Zendehnam, A., 2004. Residual stress and structural characteristics in Ti and Cu sputtered films on glass substrates at different substrate temperatures and film thickness. Phys. B: Condens. Mat. 349, 44–55.

Shoesmith, D.W., Hardie, D., Ikeda, B.M., Noel, J.J., 1997. Hydrogen absorption and lifetime performance of titanium waste containers. Atomic Energy of Canada Limited Report, AECL-11770, COG-97-035-I.

Shoesmith, D.W., Ikeda, B.M. LeNeveu, D.M., 1997. Modeling the failure of nuclear waste containers. Corrosion (Houston) 53, 820–829.

Singh, P., Kaur, D., 2008. Influence of film thickness on texture and electrical and optical properties of room temperature deposited nanocrystalline V_2O_5 thin films. J. Appl. Phys. 103 (043507), 1–9.

Siva Rama Krishna, D., Sun, Y., 2005. Effect of thermal oxidation conditions on tribological behaviour of titanium films on 316L stainless steel. Surf. Coat. Technol. 198, 447–453.

Sonoda, T., Watazu, A., Zhu, J., Shi, W., Kato, K., Asahina, T., 2004. Structure and mechanical properties of pure titanium film deposited onto TiNi shape memory alloy substrate by magnetron DC sputtering. Thin Solid Films 459, 212–215.

Textor, M., Sittig, C., Frauchiger, V., Tosatti, S., Brunette, D.M., 2001. Titanium in Medicine. Springer, Berlin, p. 172–230.

Thompson, C.V., 2000. Structure evolution during processing of polycrystalline films. Ann. Rev. Mater. Sci. 30, 159–190.

Thornton, J.A., 1977. High rate thick film growth. Ann. Rev. Mater. Sci. 7, 239–260.

Vijaya, H.S., Muralidhar, G.K., Subbanna, G.N., Mohan Rao, G., Mohan, S., 1996. Characterization of titanium thin films prepared by bias assisted magnetron sputtering. Metall. Mater. Trans. 27B, 1057–1060.

Warren, B.E., Biscce, J., 1938. Structure of silica glass by X-ray diffraction studies. J. Am. Ceram. Soc. 21, 49–54.